



Optimal Temperature Thresholding in Passive Thermography for Head and Neck Cancer Diagnosis

Ruchika Thukral^{1*}, Ashwani Kumar Aggarwal¹, A. S. Arora¹, Tapas Dora², Sankalp Sancheti³

¹Electrical and Instrumentation Engineering, Sant Longowal Institute of Engineering Technology, Longowal, Sangrur, 148106, Punjab, India.

²Department of Radiation Oncology, Homi Bhabha Cancer Hospital Research Centre RC, A Unit of Tata Memorial Centre, Mumbai Dept. of Atomic Energy [Govt. of India], Sangrur, 148001, Punjab, India.

³Department of Pathology, Homi Bhabha Cancer Hospital Research Centre, A Unit of Tata Memorial Centre, Mumbai Dept. of Atomic Energy [Govt. of India], Sangrur, 148001, Punjab, India.

*Corresponding author(s). E-mail(s): engg.ruchika@gmail.com; Contributing authors: ajatsliet@yahoo.com; ashwani.ist@sliet.ac.in; dr.tapasdora.scb.ctc@gmail.com; sankalpsancheti123@rediffmail.com;

Volume 6, Issue 10, 2024

Received: 19 March 2024

Accepted: 20 April 2024

Published: 10 May 2024

[doi:10.33472/AFJBS.6.10.2024.4213-4225](https://doi.org/10.33472/AFJBS.6.10.2024.4213-4225)

Abstract— Head and Neck Squamous Cell Carcinomas (HNSCC) is one of the major types of head and neck cancers. The diagnosis, staging, and radiotherapy planning of HNSCC is usually done using PET, CT, MRI, among many others. Due to the inherent limitations of using these imaging modalities, thermal imaging of head and neck cancer has shown significant attention during the past decade. However, the challenge lies in using thermal images of head and neck suspected patients, partly due to the lack of benchmark datasets, and nascent technology used for the analysis of thermal images. This study utilizes thermal data obtained from adult patients with suspected head and neck cancers using a FLIR-E60 thermal camera at Homi Bhabha Cancer Hospital (HBCH), Sangrur, Punjab, a unit of TATA MEMORIAL CENTRE. The proposed methodology employs optimal temperature thresholding to automatically identify and highlighting the cancerous regions from surrounding tissues, enhancing visualization by eliminating background noise and highlighting malignant areas. Mean temperatures were found to be significantly elevated in malignant tumors compared to benign ones ($37.0 \pm 1.2^\circ\text{C}$ and $33.5 \pm 1.8^\circ\text{C}$, respectively; $p=0.01$), with a temperature threshold above 34.5°C demonstrating a correlation with malignancy (sensitivity 76%, specificity 80%; $p=0.01$). Thermographic evaluation contributes to early cancer detection and aids in prognostic assessment for patients.

Keywords—Computer aided diagnosis, Head and Neck cancer detection, Image Processing, Infrared Imaging, Thresholding.

I. INTRODUCTION

The early diagnosis of head and neck cancer (commonly known as H.N.C) helps the radiation oncologists in treatment planning [1]. The risk factors associated with H.N.C are smoking [2], alcohol consumption [3], and human papillomavirus (HPV) [4], etc. The risk of developing laryngeal cancer is more than that of the pharyngeal cancer in patients with excessive smoking habits [5]. The alcohol consumption increases the risk of developing pharyngeal cancer more than that of the laryngeal cancer [6]. The tonsillar cancer is found more frequently in HPV infected patients [7]. The diagnosis of H.N.C begins with the physical examination of the patients followed by the pathology tests. The patients suspected with head and neck cancer during the physical examination and from the pathology test reports are usually undergone with an endoscopy procedure to visualize the inner lining of tissues [8]. Subsequently, the imaging techniques are used to find the cancerous cells and to assess the site of cancer. The biopsy procedure is recommended for patients with high risk factors, adverse reports of preliminary examination, and unfavourable results obtained from the imaging modalities.

The physical examination includes observation (patches in the mouth, swelling of the neck, and nose bleeding, etc.) [9], palpation (tonsillar fossa, jaw joints, and thyroid gland, etc.) [10], auscultation (cervical, cranial, and continuous arterial murmurs, etc.) [11], and percussion (maxillary sinus, sphenoid sinus, and occasionally frontal sinus, etc.) [12]. The common symptoms of H&N cancer include ear pain [13], change in voice [14], sore in mouth [15], and lump in the neck [16], etc. In addition, leukoplakia (white patches in the mouth) [17], erythroplakia (red patches in the mouth) [18], and difficulty in swallowing [19] are the important signs of H&N cancer which are useful in the diagnosis. For patients progressing to head and neck squamous cell carcinoma (HNSCC), erythroplakia is more likely to occur than leukoplakia [20]. The sign of nose bleeding alone is rarely detected in case of paranasal sinus cancer, which is one of the major types of H&N cancer [21].

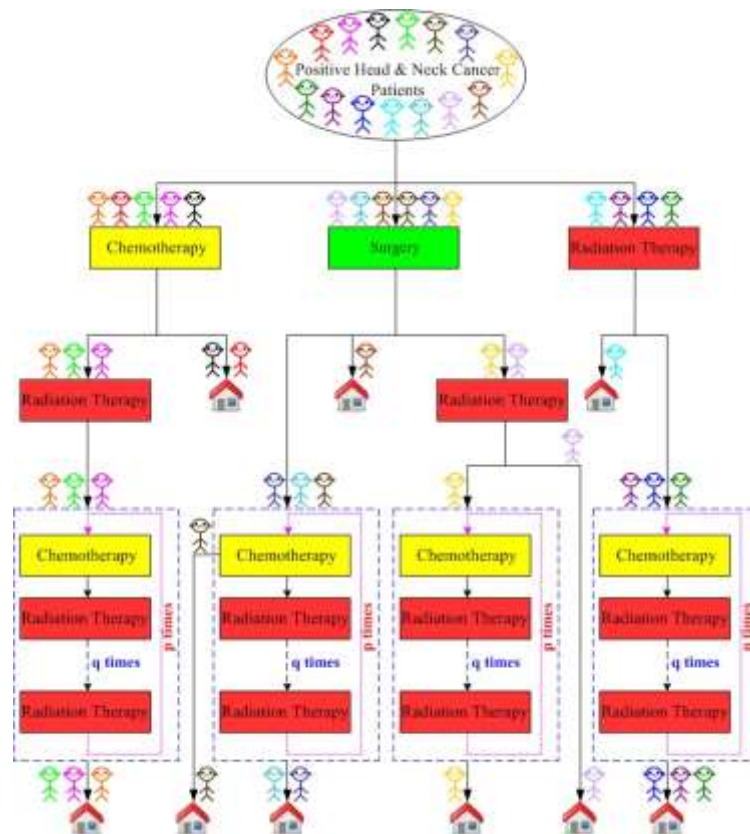


Figure 1: Treatment options for H.N.C patients

The pathology tests include a complete blood count (CBC), blood typing, and enzyme analysis. The CBC examines the number of red blood cells, white blood cells, and platelets. The endoscopy of the patients suspected with head and neck cancer helps to find the malignant cells and to determine the extent of the tumor. The commonly used imaging modalities viz. X-rays, panoramic radiograph, computed tomography (CT), positron emission tomography (PET), ultrasound, and magnetic resonance imaging (MRI), etc. are proved to be useful tools in the diagnosis of H.N.C. In biopsy, a sample tissue is collected from the tumor or lymph node using a fine needle aspiration [22]. The collected sample tissue is investigated under an electron microscope by a pathologist for cytologic examination. The digitized microscopic images (whole slide images) are analyzed using standard software such as Digital Imaging and Communications in Medicine (DICOM) or customized machine learning models. The biopsy is sometimes combined with biomarkers in order to identify either the specific genes (*NOTCH1*, *ALDH2*, *SDHD*, and *SDHB*, etc.), or specific proteins (*salivary*, *IL-6*, *IL-8*, *MMP-9*, *chemerin*, *Naalop*, *CEA*, *Cyfra21-1*, and *angiogenic factor*, etc.) for genetic testing [23].

Although, the imaging modalities, biopsy, whole slide imaging, and biomarker testing are the useful tools for diagnosis, nevertheless each of these methods suffer from one drawback or the other. For instance, MRI is a preferred imaging modality for soft tissues such as tonsils, torn ligaments, and base of tongue, however a contrast medium needs to be injected into the patient's body which might not be convenient or might have complications in some cases [24]. Furthermore, MRI is an expensive instrument which might not be available in many diagnostic centers. Another approach known as (*bone scan*) is often used for the task, however specific radioactive traces such as tritium, carbon-11, carbon-14, oxygen-14, fluorine-18, phosphorous-32, sulfur-35, technetium-99, iodine-123, and gallium-67, etc. must be injected into the vein in order to obtain high contrast image of the organ [25]. The treatment planning is a crucial step that depends on various factors such as age, medical history, and physical condition of the patient. Figure 1 shows the treatment options for the head and neck cancer patients that include surgery, radiation therapy, chemotherapy, and a combination of these treatments.

Considering the limitations and the difficulties in the use of above-mentioned diagnostic methods; a non-invasive, portable, and inexpensive imaging modality, namely the thermal imaging, also known as thermography, has become a preferable diagnostic modality since the last two decades [26]. This is partly due to advancement in the sensor technology and the availability of fast computational methods [27]. The thermal imaging is based on the concept of heat map which is generated due to variations in the energy (E) of infrared radiation emitted per unit area per unit time by the human body according to Stefan-Boltzmann law as given in equation (1).

$$E = \sigma \epsilon T^4 \quad (1)$$

where, σ is called Stefan-Boltzmann constant and its value is $5.67037 \times 10^{-8} \text{Wm}^{-2}\text{K}^{-4}$. ϵ is the emissivity of human skin with a typical value of 0.98 (unitless). T is the absolute temperature of the human body in Kelvin. The maximum wavelength (λ_{max}) of the IR radiation emitted by a body at absolute temperature T follows Wien's displacement law which is given by equation (2).

$$\lambda_{\text{max}} = \frac{b}{T} \quad (2)$$

where, $b=2898 \mu\text{m}$ is Wien's displacement constant. The typical values for the wavelength of IR radiation emitted by the body at various temperatures is enumerated in Figure 2.

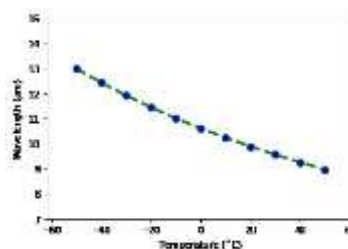


Figure 2: Effect of temperature on wavelength of emitted thermal radiation

It is observed that the objects emit radiation in mid IR wavelength range for temperature between $-50\text{ }^{\circ}\text{C}$ to $+50\text{ }^{\circ}\text{C}$. Infrared region of the electromagnetic spectrum in the wavelength range from $1\text{ }\mu\text{m}$ to $14\text{ }\mu\text{m}$. The thermal imaging methods are divided into two types. One is the passive thermography in which a heat map is generated from thermal radiations emitted from the body and another is the active thermography in which the subject is exposed to stimulus (heat or cold). Thermal imaging offers a visual representation of the thermal characteristics of the affected skin area. By employing appropriate processing techniques, quantitative data can be compared and associated with various disease conditions, automating the detection of cancers. In medical thermography, abnormalities can be visually diagnosed through thermograms, but accurately quantifying thermal patterns necessitates objective analysis approaches for regions of interest (ROIs). This study aims to identify heat patterns within ROIs, interpreting the presence of malignancy by analysing the prominence of red color relative to other hues, potentially indicating thermal characteristics of cancerous lesions.

II. MATERIALS AND METHODS

The dataset used in this paper consists of thermal images taken with FLIR E-60 thermal camera from head and neck cancer suspected patient. The dataset of thermal images of the head and cancer patients were taken from Homi Bhabha Cancer Hospital (HBCH) Sangrur, Punjab –A Unit of TATA MEMORIAL CENTRE, IEC, A Grant-in-Aid Institution Under Department of Atomic Energy. Govt. of India.

A. Dataset Used

The thermal images are captured using FLIR E-60 thermal camera, the images are in the standard JPEG format with a spatial resolution of $320\text{ X }240$. Each of the images is 3-channel RGB image with 8-bit pixel depth. For quality assurance in clinical thermal imaging and for patient safety, standard protocols for thermal imaging have been used while capturing the thermal data. The protocols include clinical settings, instructions to the patients, safety protocols, and infrastructural facilities, etc.

- **Clinical Settings:** The appropriate clinical settings are necessary in order to obtain high contrast, accurate, and reliable thermal images of the patients. The room design and the environmental control are the important aspects of clinical settings. The room in which the data is collected has a size with dimensions of 8 meter (width) X 6 meter (length) X 3 meter (height). The adequate lighting conditions were maintained using standard fluorescent lamps. There was no incandescent lamp in the room as the incandescent lamps use a tungsten filament that emits IR radiations which may interfere with the thermal camera. The heating ducts and the air conditioning vents were kept away from the patient while taking the thermal images.
- **Instructions to the Patients:** A set of instructions were conveyed to the patients prior to the imaging procedure. The patients were instructed to avoid long sun exposure or sun bathing five days prior to visiting the clinic for thermal imaging. The use of foundation, body lotion, deodorants, other cosmetic products were prohibited on the day of imaging. The ornaments such as necklace, earrings, nose pins, etc. were also prohibited. The patients wearing contact lenses, eye glasses, or spectacles were asked to remove them during the scanning process.
- **Safety Protocols:** As the data has been collected during the covid pandemic, the covid safety protocols were also used along with general clinical safety protocols such as hygiene, proper shielding, sterilization of equipment, and use of floor disinfectant, etc.
- **Infrastructural Facilities:** The imaging room was equipped with humidity monitor, indoor thermometer, and patient monitoring equipment. The wheelchair, ramp, handrail, and braille facilities were available for people with disabilities. The common facilities such as elevator, ambulance service, drinking water, waiting area, restrooms, and nursing room were also available.

B. Infrared Imaging Protocols

Before the thermographic examination, patients were instructed to abstain from alcohol, caffeine, physical exercise, and nicotine for a minimum of two hours. Room temperature was maintained within the range of $20\text{ }^{\circ}\text{C}$ to

23°C, as per the standard thermal imaging protocols. Prior to the examination, patients were required to remove earrings, necklaces, or any other accessories. Positioned in front of the camera, the patient's distance from it was standardized to approximately 1 meter, although variations from 0.8 meters to 1.2 meters were permitted, contingent upon the patient's size. Parameters such as distance, room temperature, and relative air humidity were meticulously recorded and inputted into the FLIR-E60 thermal camera.

C. Study Design

The study was designed to assist the oncologist in deciding the appropriate dose and treatment procedure based on the extracted cancerous region at an early stage, hence improving the quality of life after treatment. No person will be harmed physically, emotionally, psychologically, financially, or in any other way during this data collection. The study employed inclusive eligibility criteria, encompassing patients who underwent radiotherapy, with or without chemotherapy, for head and neck cancers. Participation was voluntary, with individuals exercising their autonomy in deciding whether to partake. Approval for the research was secured from the Tata Memorial Centre. All participants provided written consent, receiving a copy of the Informed Consent Form for their records. The study exclusively included adults as its primary demographic. The study applied exclusive criteria, omitting studies that met certain conditions: It excluded studies involving children (less than 18 years) and pregnant women, as well as patients with psychological illnesses. Additionally, individuals who were unwilling to sign the informed consent form were not included in the analysis.

III. PROPOSED METHODOLOGY

The thermal images were captured using a thermal camera from H.N.C patients over a span of three months. A total of 130 such patients were pre-screened with H.N.C using several pre-screening methods for cancer diagnosis such as CT scan and preliminary examination by radiologist. The thermal imaging was carried under control conditions such as ambient temperature, humidity, and other distractions. Each patient was asked to refrain from alcohol consumption, smoking, and regressive exercise at least 24 hours prior to capturing the thermal images. Thermal camera was placed at a distance of 1m away from the patient’s body to capture the thermal images. The size of the thermal image captured by the camera was adjusted to 320 X 240 with bit depth to 8 bits per pixel. Image processing techniques are required to visualize the region's geometry of interest better to eliminate the background interference from thermograms. In this research, an interactive method for optimal threshold is proposed to convert a grey- level thermogram into a binary image. The proposed methodology is depicted in Figure 3.

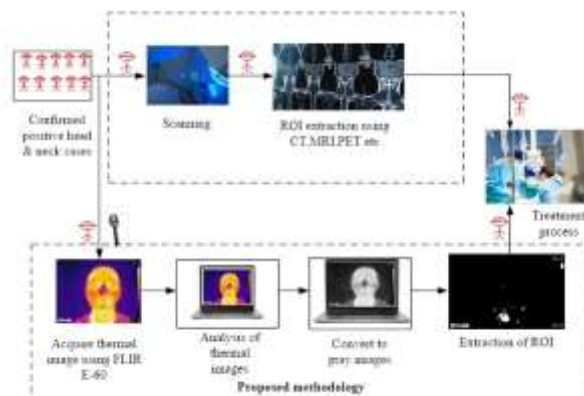


Figure 3: Proposed Methodology for ROI Extraction

The thermal images produced from the thermal camera are further analysed and processed to reveal the primary location of the malignancy, which is then validated using standard imaging modalities such as histopathology findings, CT scans, PET scans, and so on. In this research, an interactive method for optimal

threshold is proposed to convert a grey-level thermogram into a binary image. This process is performed in the steps illustrated in Algorithm 1.

Algorithm 1 - Optimal temperature thresholding

Require: T_{max} and T_{min} are the maximum and minimum temperatures of the thermogram image.

Maximum iteration number $N=100$, Tolerance $T_{ol}=0.001$

The initial value for temperature threshold

$$T_1 = \frac{T_{max} + T_{min}}{2}$$

and $T_2 = T_1 + 1$.

Variance of thermal image σ^2 , probability of foreground $P_f=0.6$, probability of background = $P_b=0.4$

Step 1: for $i=1$ to N do

Step 2: If $T_{i+1} - T_i < T_{ol}$; Terminate

Step 3: Background image,

$$I_b = \begin{cases} 1 & I < T_i \\ 0 & \text{else} \end{cases}$$

Step 4: Foreground image,

$$I_f = \begin{cases} 1 & I \leq T_i \\ 0 & \text{else} \end{cases}$$

Step 5: Average temperature μ_b and μ_f of regions I_b and I_f , respectively.

Step 6: $T_{i+1} = \frac{T_{max} + T_{min}}{2} + \frac{\sigma^2}{\mu_b - \mu_f} + \ln\left(\frac{P_f}{P_b}\right)$

Step 7: end

By using temperature thresholding technique, the gray-level thermograms were transformed into binary images, where the ROIs were showed with white color, as revealed in Figure 4. Thresholding offers improved visualization by removing the background interference and highlighting the cancerous region separately.

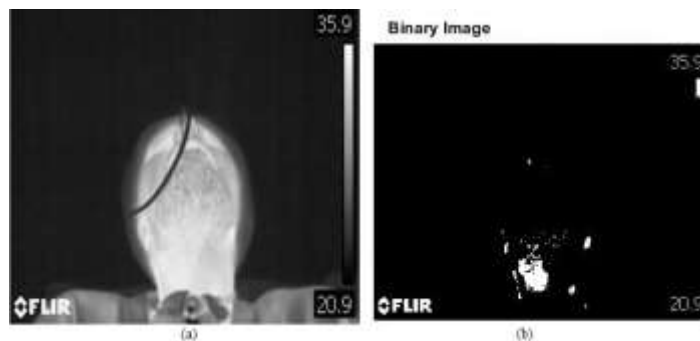


Figure 4: Illustrates the outcome of thresholding method (a) Gray-level thermogram (b) binary mask of thermogram achieved after thresholding technique

This image segmentation technique used to automatically determine the optimal threshold for image binarization. It aims to maximize the inter-class variance between foreground and background pixels, effectively separating them into two distinct classes. This method begins by computing a histogram of pixel intensity values in the grayscale image. Then, it iterates through all possible threshold values and calculates the weighted sum of variances for the two classes formed by the threshold. The threshold that maximizes this inter-class variance is selected as the optimal threshold for binarization. Overall, thresholding method offers a simple yet powerful approach for automated image segmentation, providing a robust solution for various image analysis tasks.

IV. RESULTS AND DISCUSSION

Oral cavity cancer is a significant and rising concern. Patients with a single metastatic lymph node on both sides had a 25% worse survival probability than those who did not have lymph node metastasis. Thus, the assessment and proper management of cancerous patient treatment is crucial and one of the challenges to the researchers. Thermal imaging provides a visual interpretation of the thermal properties of the affected skin area. With suitable processing techniques, comparison and association of quantitative data with diseases of interest can automate the detection of various cancer conditions. In medical thermography, the abnormalities can be diagnosed by visual inspections of thermograms, but the accurate and reliable quantification of thermal patterns demands the approaches for objective analysis of ROIs [10]. This work aimed to identify heat patterns from ROIs to interpret the presence of malignancy by studying and analysing the prominence of red color compared to its counterparts, which could indicate thermal tendencies of cancerous lesions.

Marking the hot spot in thermal imaging is a critical step in diagnosing cancer, especially for detecting H.N.C. This process involves identifying areas on the thermal image that exhibit higher temperatures compared to surrounding tissues, indicating increased metabolic activity often associated with cancerous growths. The procedure begins with acquiring high-resolution thermal images of the patient's head and neck using a thermal camera, which captures temperature variations across the skin surface. These images are then pre-processed to enhance quality and reduce noise, employing filtering techniques and contrast adjustments to ensure clear differentiation between normal and abnormal regions.

An optimal temperature threshold is determined using methods, which distinguishes the hot spot from the background by segmenting the image into regions with temperatures above and below the threshold. Regions exceeding the threshold are identified and marked as hot spots, visually highlighted on the thermal image for easy identification, often through circles or annotations. These marked hot spots are analysed for their location, size, and intensity, and oncologists interpret these findings to assess the likelihood of cancer. The presence of a hot spot in specific areas prone to tumors can be a significant indicator of malignancy.

The thermal imaging results are then correlated with other clinical data, such as physical examinations, patient history, and additional diagnostic tests like MRI or CT scans. This comprehensive analysis helps confirm the diagnosis and plan further treatment. In Figure 5 and Table 2, the hot spot identified through this process is clearly marked, providing a visual cue for medical professionals. This marked hot spot is a crucial piece of evidence in the diagnostic workflow, aiding in the early detection and treatment of cancer. Precision in marking and interpreting these hot spots can significantly impact the prognosis and treatment outcomes for patients. Some of the common segmentation algorithms are the graphic cut method, region growth method, active contour method, and level set method. When outlining

the region of interest of a tumor, it is necessary to pay attention to whether the image needs to be aligned, as the ROI is generally small in size [11].

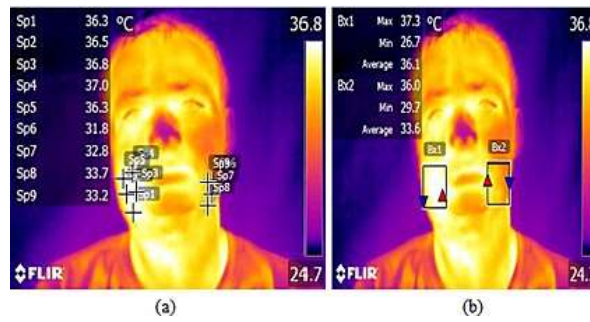


Figure 5: Marking the hot spots in the thermal image

Table 1: Shows the asymmetry on both sides

S. No	Right Side	Left Side	Remarks
1.	Sp1: 36.3°C	Sp8: 33.7°C	H.N.C patient Site: Right Buccal Mucosa, Stage: IV(B), Clinically Node: 0
2.	Sp2: 36.5°C	Sp7: 32.8°C	
3.	Sp5 :36.3°C	Sp9: 33.2°C	
4.	Sp4: 37.0°C	Sp6: 31.8°C	
5.	Max: 37.3°C	Max: 36.0°C	
6.	Min: 26.7°C	Min: 29.7°C	
7.	Average: 36.1°C	Average: 33.6°C	

Subject	Temp. on Right side	Temp. on Left side	Temp. profile on cancerous region	Temp. profile on normal region	Site of cancer
1	Sp2- 34.3°C Sp4- 34.4°C	Sp1- 37°C Sp3- 36.8°C	Max.-37.1°C Min.- 35.2°C Avg.- 36.5°C	Max.- 34.8°C Min.- 30.6°C Avg.- 33.2°C	Left
2	Sp1- 37.1°C Sp3- 37°C	Sp2- 34°C Sp4- 33.6°C	Max.-37.1°C Min.- 35.7°C Avg.- 36.6°C	Max.- 35.7°C Min.- 27.9°C Avg.- 33.2°C	Right
3	Sp2- 32.3°C Sp4- 32.7°C	Sp1- 35.2°C Sp3- 35°C	Max.-35.7°C Min.- 26.6°C Avg.- 34.7°C	Max.- 34.3°C Min.- 23.9°C Avg.- 31.2°C	Left
4	Sp2- 32.4°C Sp4- 33.1°C	Sp1- 35.7°C Sp3- 35.6°C	Max.-35.9°C Min.- 33.9°C Avg.- 35°C	Max.-34.9°C Min.- 31.4°C Avg.- 33.1°C	Left
5	Sp2- 33.4°C Sp4- 32.3°C	Sp1- 34.6°C Sp3- 34.5°C	Max.-35.6°C Min.- 31.4°C Avg.- 33.5°C	Max.-34.7°C Min.- 26.1°C Avg.- 32°C	Left
6	Sp2- 33.9°C Sp4- 33.1°C	Sp1- 35.4°C Sp3- 34.9°C	Max.-36.2°C Min.- 32.2°C Avg.- 34.1°C	Max.-34.2°C Min.- 30.8°C Avg.- 32.5°C	Left
7	Sp1- 36.4°C Sp3- 35.8°C	Sp2- 33.9°C Sp4- 33.7°C	Max.-37°C Min.- 33.8°C Avg.- 36.1°C	Max.-35.1°C Min.- 32.6°C Avg.- 34.1°C	Right
8	Sp2- 34.8°C Sp4- 34°C	Sp1- 36°C Sp3- 35.8°C	Max.-36.5°C Min.- 34°C Avg.- 35.3°C	Max.-35°C Min.- 32.5°C Avg.- 33.6°C	Left

9	Sp2- 34.2°C Sp4- 34.1°C	Sp1- 36.5°C Sp3- 36.4°C	Max.-36.7°C Min.- 34.7°C Avg.- 36.3°C	Max.-35.2°C Min.- 29.2°C Avg.- 34.3°C	Left
10	Sp1- 34.6°C Sp3- 33.9°C	Sp2- 31.7°C Sp4- 30.1°C	Max.-35.2°C Min.- 32.6°C Avg.- 34.1°C	Max.-34.2°C Min.- 27.4°C Avg.- 31.6°C	Right

The optimal temperature thresholding method for Region of Interest (ROI) extraction is a crucial step in thermal imaging analysis, particularly in medical applications such as cancer diagnosis. This method involves identifying temperature thresholds that delineate areas of interest, such as potential tumor sites, from background tissue in thermographic images. To determine these thresholds, various statistical and computational techniques are employed. One common approach is to calculate statistical measures such as mean and standard deviation of temperature values within the image. Based on these statistics, a threshold temperature can be determined, beyond which pixels are classified as part of the ROI. Another method involves using histogram analysis to identify distinct temperature distributions corresponding to different tissue types, with thresholds selected accordingly. The selection of the optimal temperature threshold is critical as it directly impacts the accuracy of ROI extraction. Setting the threshold too low may result in including irrelevant regions, leading to false positives, while setting it too high may lead to missing important areas, resulting in false negatives. Therefore, careful calibration and validation of the thresholding method are essential to ensure accurate and reliable ROI extraction.

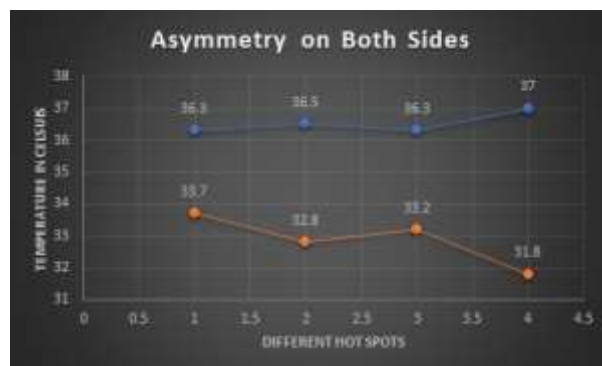


Figure 6: Cancer leads to an increase in temperature

Cancer leads to an increase in temperature, a phenomenon observed in thermal imaging. This rise in temperature is due to the higher metabolic activity of cancerous cells, which require more energy and, consequently, generate more heat compared to normal cells. The localized increase in temperature can serve as an indicator of malignancy, making thermal imaging a valuable tool in the early detection and diagnosis of cancer. By identifying areas with elevated temperatures, medical professionals can pinpoint potential tumor sites and assess the extent of the disease, aiding in the formulation of effective treatment plans. Figure 6 illustrates that cancer leads to an increase in temperature. Moreover, advancements in image processing techniques, such as machine learning algorithms, have been increasingly utilized to optimize temperature thresholding for ROI extraction. These techniques enable the automated learning of optimal thresholds from training data, improving the efficiency and accuracy of the extraction process.

Overall, the optimal temperature thresholding method plays a crucial role in extracting meaningful information from thermographic images, particularly in medical contexts where precise delineation of ROIs is essential for diagnosis and treatment planning. Continued research and development in this area are essential to further enhance the accuracy and efficiency of ROI extraction techniques.

This method does not require any prior knowledge about the image or manual tuning of parameters. It is particularly effective in scenarios where the histogram of pixel intensities exhibits distinct peaks corresponding to different image regions, making it suitable for a wide range of applications, including medical imaging, document processing, and object recognition. This method not perform optimally in cases where the foreground and background distributions overlap significantly or when the image contains noise. In such situations, preprocessing techniques or alternative thresholding methods may be necessary to improve segmentation accuracy.

V. CONCLUSION

Infrared thermal imaging has recently attracted the attention of a variety of research to find solutions to the issues in a larger area of medicine and engineering fields. It has been used to detect various abnormalities in which increased or decreased skin temperature specifies the existence of reduced blood flow related to physiological abnormalities. Thermal imaging is ideal for medical diagnostics when patient care is considered non-invasive and non-ionizing. CT scans, X-ray scans, mammography, and magnetic resonance imaging are well-equipped medical imaging procedures to evaluate the anatomy and diagnosis of different parts of the human body. On the other hand, these methods are based on radiation and are hazardous to humans. With recent improvements in sensor technology and analysis tools, the time required to capture a thermal image, pre-process it and evaluate it has reduced significantly over the last few decades. The computational time of the optimal thresholding method is 0.178226 seconds. Recent advancements and research in thermal imaging applications have shown encouraging results. As a result, more research and development of thermography procedures as a health and diagnostic tool in the framework of precancerous stage diagnosis is required.

References

- [1] F. Linkov, A. Lisovich, Z. Yurkovetsky, A. Marrangoni, L. Velikokhatnaya, B. Nolen, M. Winans, W. Bigbee, J. Siegfried, A. Lokshin et al., "Early detection of head and neck cancer: development of a novel screening tool using multiplexed immunobead-based biomarker profiling," *Cancer Epidemiology Biomarkers & Prevention*, vol. 16, no. 1, pp. 102–107, 2007.
- [2] K. Kobayashi, K. Hisamatsu, N. Suzui, A. Hara, H. Tomita, and T. Miyazaki, "A review of hpv-related head and neck cancer," *Journal of clinical medicine*, vol. 7, no. 9, p. 241, 2018.
- [3] H. Maier, A. Dietz, U. Gewelke, W. Heller, and H. Weidauer, "Tobacco and alcohol and the risk of head and neck cancer," *The clinical investigator*, vol. 70, no. 3, pp. 320–327, 1992.
- [4] S. Marur, G. D'Souza, W. H. Westra, and A. A. Forastiere, "Hpv associated head and neck cancer: a virus-related cancer epidemic," *The lancet oncology*, vol. 11, no. 8, pp. 781–789, 2010.
- [5] J. H. Lubin, M. M. Gaudet, A. F. Olshan, K. Kelsey, P. Boffetta, P. Brennan, X. Castellsague, C. Chen, M. P. Curado, L. D. Maso et al., "Body mass index, cigarette smoking, and alcohol consumption and cancers of the oral cavity, pharynx, and larynx: modeling odds ratios in pooled case-control data," *American journal of epidemiology*, vol. 171, no. 12, pp. 1250–1261, 2010.

- [6] D. Kawakita and K. Matsuo, "Alcohol and head and neck cancer," *Cancer and Metastasis Reviews*, vol. 36, no. 3, pp. 425–434, 2017.
- [7] D. Lindquist, M. Romanitan, L. Hammarstedt, A. Nasman, " H. Dahlstrand, J. Lindholm, L. Onelov, T. Ramqvist, W. Ye, " E. Munck-Wikland et al., "Human papillomavirus is a favourable prognostic factor in tonsillar cancer and its oncogenic role is supported by the expression of e6 and e7," *Molecular oncology*, vol. 1, no. 3, pp. 350–355, 2007.
- [8] M. Halicek, M. Shahedi, J. V. Little, A. Y. Chen, L. L. Myers, B. D. Sumer, and B. Fei, "Head and neck cancer detection in digitized whole slide histology using convolutional neural networks," *Scientific reports*, vol. 9, no. 1, pp. 1–11, 2019.
- [9] M. N. Prout, J. N. Sidari, R. A. Witzburg, G. A. Grillone, and C. W. Vaughan, "Head and neck cancer screening among 4611 tobacco users older than forty years," *Otolaryngology–Head and Neck Surgery*, vol. 116, no. 2, pp. 201–208, 1997. [10] H. K. Walker, W. D. Hall, and J. W. Hurst, "Clinical methods: the history, physical, and laboratory examinations," 1990.
- [11] "AUSCULTATION OF HEAD AND NECK," *JAMA*, vol. 183, no. 8, pp. 684–685, 02 1963. [Online]. Available: <https://doi.org/10.1001/jama.1963.03700080092023>
- [12] L. Dooley and J. Shah, "Management of the neck in maxillary sinus carcinomas," *Current opinion in otolaryngology & head and neck surgery*, vol. 23, no. 2, p. 107, 2015.
- [13] T. J. Scarbrough, T. A. Day, T. E. Williams, J. H. Hardin, E. G. Agüero, and C. R. Thomas Jr, "Referred otalgia in head and neck cancer: a unifying schema," *American journal of clinical oncology*, vol. 26, no. 5, pp. e157–e162, 2003.
- [14] C. E. Moore and F. Durden, "Head and neck cancer screening in homeless communities: Heal (health education, assessment, and leadership)," *Journal of the National Medical Association*, vol. 102, no. 9, pp. 811– 816, 2010.
- [15] T.-Y. Liu, C.-C. Lee, H.-Y. Huang, and J.-G. Chang, "Mutation analysis of second primary tumors in the head and neck cancer by next generation sequencing," in *2018 IEEE 18th International Conference on Bioinformatics and Bioengineering (BIBE)*. IEEE, 2018, pp. 315–318.
- [16] S. Sengupta, R. Pal et al., "Clinicopathological correlates of pediatric head and neck cancer," *Journal of Cancer Research and Therapeutics*, vol. 5, no. 3, p. 181, 2009.
- [17] T. Tikka, P. Pracy, and V. Palleri, "Refining the head and neck cancer referral guidelines: a two centre analysis of 4715 referrals," *British Journal of Oral and Maxillofacial Surgery*, vol. 54, no. 2, pp. 141–150, 2016.
- [18] S. Raj, K. K. Kesari, A. Kumar, B. Rathi, A. Sharma, P. K. Gupta, S. K. Jha, N. K. Jha, P. Slama, S. Roychoudhury et al., "Molecular mechanism (s) of regulation (s) of c-met/hgf signaling in head and neck cancer," *Molecular Cancer*, vol. 21, no. 1, pp. 1–16, 2022.

- [19] A. A. Simental and R. L. Carrau, "Assessment of swallowing function in patients with head and neck cancer," *Current Oncology Reports*, vol. 6, no. 2, pp. 162–165, 2004.
- [20] K. D. Hunter, E. K. Parkinson, and P. R. Harrison, "Profiling early head and neck cancer," *Nature Reviews Cancer*, vol. 5, no. 2, pp. 127–135, 2005.
- [21] H. Shaw, "Early diagnosis of cancer in the head and neck." *British Medical Journal*, vol. 1, no. 6006, p. 379, 1976.
- [22] M. Knappe, M. Louw, and R. T. Gregor, "Ultrasonography-guided fine needle aspiration for the assessment of cervical metastases," *Archives of Otolaryngology–Head & Neck Surgery*, vol. 126, no. 9, pp. 1091–1096, 2000.
- [23] U. Landegren and M. Hammond, "Cancer diagnostics based on plasma protein biomarkers: hard times but great expectations," *Molecular Oncology*, vol. 15, no. 6, pp. 1715–1726, 2021.
- [24] D. W. Tshering Vogel and H. C. Thoeny, "Cross-sectional imaging in cancers of the head and neck: how we review and report," *Cancer Imaging*, vol. 16, no. 1, pp. 1–15, 2016.
- [25] F. L. Ampil, M. J. Wood, H. W. Chin, D. K. Hoasjoe, R. F. Aarstad, and D. L. Hilton, "Screening bone scintigraphy in the staging of locally advanced head and neck cancer," *Journal of Cranio-Maxillofacial Surgery*, vol. 23, no. 2, pp. 115–118, 1995.
- [26] R. Roslidar, A. Rahman, R. Muharar, M. R. Syahputra, F. Arnia, M. Syukri, B. Pradhan, and K. Munadi, "A review on recent progress in thermal imaging and deep learning approaches for breast cancer detection," *IEEE Access*, vol. 8, pp. 116 176–116 194, 2020.
- [27] J. M. Blackledge, *Digital image processing: mathematical and computational methods*. Elsevier, 2005.
- [28] A. Saxena, E. Ng, and S. T. Lim, "Infrared (ir) thermography as a potential screening modality for carotid artery stenosis," *Computers in Biology and Medicine*, vol. 113, p. 103419, 2019.
- [29] A. Saxena, V. Saha, and E. Y. K. Ng, "Skin temperature maps as a measure of carotid artery stenosis," *Computers in Biology and Medicine*, vol. 116, p. 103548, 2020.
- [30] R. Ren, H. Luo, C. Su, Y. Yao, and W. Liao, "Machine learning in dental, oral and craniofacial imaging: a review of recent progress," *PeerJ*, vol. 9, p. e11451, 2021.
- [31] Z. Xu, Q. Wang, D. Li, M. Hu, N. Yao, and G. Zhai, "Estimating departure time using thermal camera and heat traces tracking technique," *Sensors*, vol. 20, no. 3, p. 782, 2020.
- [32] K. Sivesgaard, L. P. Larsen, M. Sørensen, S. Kramer, S. Schlander, N. Amanavicius, F. V. Mortensen, and E. M. Pedersen, "Whole-body mri added to gadoxetic acid-enhanced liver mri for detection of extrahepatic disease in patients considered eligible for hepatic resection and/or local ablation of colorectal cancer liver metastases," *Acta radiologica*, vol. 61, no. 2, pp. 156–167, 2020.

- [33] C. Matias, T. Bordieri, D. Roberts, V. J. Cheever, L. K. Munk, M. S. Lipsky, M. D. Fahmy, and A. J. Gross, "Small molecule inhibition of matrix metalloproteinases as a potential therapeutic for metastatic activity in squamous cell carcinoma," *Oral Cancer*, vol. 3, no. 1, pp. 1–8, 2019.
- [34] S. Derruau, F. Bogard, G. Exartier-Menard, C. Mauprivez, and G. Polidori, "Medical infrared thermography in odontogenic facial cellulitis as a clinical decision support tool. a technical note," *Diagnostics*, vol. 11, no. 11, p. 2045, 2021.
- [35] M. S. Kwak, Y.-G. Eun, J.-W. Lee, and Y. C. Lee, "Development of a machine learning model for the prediction of nodal metastasis in early t classification oral squamous cell carcinoma: Seer-based population study," *Head & Neck*, vol. 43, no. 8, pp. 2316–2324, 2021.
- [36] Thukral R, Aggarwal AK, Arora AS, Dora T, Sancheti S. Artificial intelligence-based prediction of oral mucositis in patients with head-and-neck cancer: A prospective observational study utilizing a thermographic approach. *Cancer Research, Statistics, and Treatment*. 2023 Apr 1;6(2):181-90.
- [37] A. Bhowmik, B. Ghosh, M. Pal, R. R. Paul, J. Chatterjee, and S. Chakraborty, "Portable, handheld, and affordable blood perfusion imager for screening of subsurface cancer in resource-limited settings," *Proceedings of the National Academy of Sciences*, vol. 119, no. 2, p. e2026201119, 2022.
- [38] X. A. Lopez-Cortés, F. Matamala, B. Venegas, and C. Rivera, "Machine-learning applications in oral cancer: A systematic review," *Applied Sciences*, vol. 12, no. 11, p. 5715, 2022.
- [39] S. Liu, Z. Zhao, Z. Wang, T. Diao, K. Zhang, H. Zhang, D. Sun, F. Kong, and Q. Fu, "Establishing a thermal imaging technology (irt) based system for evaluating rat erectile function," *Sexual Medicine*, vol. 10, no. 1, p. 100475, 2022.
- [40] F. Dong, C. Tao, J. Wu, Y. Su, Y. Wang, Y. Wang, C. Guo, and P. Lyu, "Detection of cervical lymph node metastasis from oral cavity cancer using a non-radiating, noninvasive digital infrared thermal imaging system," *Scientific Reports*, vol. 8, no. 1, pp. 1–9, 2018.